

## METHOD

B. V. Naumov, O. G. Shakhrai,  
and V. I. Éiduk

UDC 532.507

1. Instruments whose operation is based on schlieren methods for visualizing transparent inhomogeneities are increasingly widely used for studying turbulence [1-3]. Various modifications of schlieren instruments make use of viewing diaphragms with stepped changes in the transmission or optical thickness [4, 5]. Extensive use of schlieren instruments in aerodynamic [6], ballistics [7], and oceanographical [1] experiments is inhibited by the susceptibility of the instruments to the effect of destabilizing factors: vibrations, temperature and pressure differentials, which displace the optical axes of the primary elements relative to the viewing diaphragm, leading to a corresponding increase in the measurement errors. Instruments constructed according to special schemes for protection against vibrations [8] are more stable with respect to the action of external factors, but instruments that make use of the direct schlieren method of visualization are more effective [9]: it is almost totally free of the disadvantage indicated due to the absence of viewing diaphragms. The direct schlieren method is successfully used, for example, in oceanographical investigations of convective turbulence, "salt fingers," as well as in ballistics experiments [10, 11, 7].

In analyzing the results of investigations of turbulent fields, it is necessary to know the sensitivity and frequency selection properties of the instruments. The effect of the viewing method on the spectrum of the output signal is examined in [7] within the geometric optics approximation. However, for many problems, it is of interest to have a more exact analysis of the sensitivity and frequency selection properties of the instruments, carried out with the use of diffraction theory. The present work is concerned with solving this problem in application to the direct schlieren method for visualizing turbulent fields.

2. At the present time, in describing interference methods of visualization (schlieren and direct schlieren) the input actions are characterized by different parameters (path length difference, gradient of the refractive index, and derivative of the gradient of the refractive index, respectively), which makes it difficult to compare the methods. Since the methods are intended for observing phase objects, it is useful to introduce a universal characteristic of the form

$$H(\xi, \eta) = K(\xi, \eta) / \Phi_m(\xi, \eta), \quad (2.1)$$

for estimating the sensitivity and spatial-frequency properties of the methods (and instruments constructed based on these methods). Here  $K(\xi, \eta)$  is the contrast of the image of a sinusoidal phase grating with spatial frequencies  $\xi$  and  $\eta$ ;  $\Phi_m(\xi, \eta)$  is the amplitude of modulation of the phase of the light wave passing through the grating.

The characteristic (2.1) is similar to the contrast-frequency characteristic that is widely used for describing the properties of optical systems for observing amplitude objects [12, 13] and represents the factor for converting phase modulation into intensity modulation for different spatial frequencies, i.e., it is a phase contrast-frequency characteristic (PCFC). In order to determine the PCFC, it is necessary to find the contrast of the image of a two-dimensional phase grating

$$t(\vec{x}) = \exp[i\Phi(\vec{x})] = \exp\left[j\Phi_m \cos 2\pi\left(\frac{\cos \alpha}{\Lambda}x + \frac{\cos \beta}{\Lambda}y\right)\right], \quad (2.2)$$

where  $\cos \alpha = \Lambda\eta$ , and  $\cos \beta = \Lambda\xi$  are the directional cosines of the propagation vector  $\vec{r}$ ;  $\Lambda$  is the spacing of the phase grating (Fig. 1, which shows the path of the rays in the optical

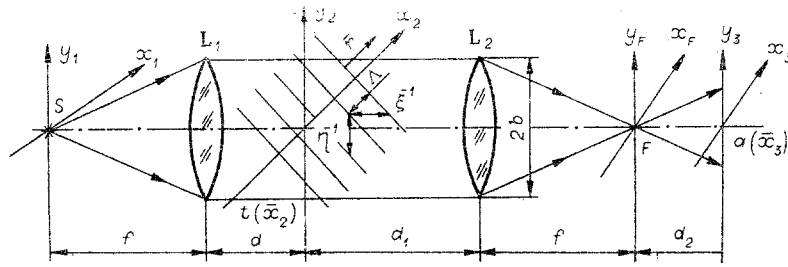


Fig. 1

system that realizes the direct schlieren method; S is the source of radiation; L<sub>1</sub> and L<sub>2</sub> are objectives for the emitting and receiving parts of the system, between which the volume being examined is positioned; x<sub>F</sub> and y<sub>F</sub> are the coordinates in the focal plane of the objective L<sub>2</sub>; x<sub>3</sub> and y<sub>3</sub> are the coordinates of the observation plane).

If the optical system has circular symmetry, the contrast does not depend on the angle of rotation of the grating relative to the optical system and in order to analyze the properties of the system it is sufficient to use a one-dimensional grating  $t(x_2) = \exp j\Phi_m \cos 2\pi x_2$ .

PCFC is introduced analytically by transforming the amplitude of the light field in the optical system (Fig. 1) in the paraxial approximation using the function  $\Psi(x, y, F) = \exp \left[ -j \frac{\pi}{\lambda} \cdot p(x^2 + y^2) \right]$  [14]. Assuming that the lenses L<sub>1</sub> and L<sub>2</sub> are thin and using successive transformations corresponding to the transmission of a wave emitted by a point monochromatic source S through the elements of the optical system and the space between them, it is possible to obtain the following expression for the amplitude of the field in the image plane (a constant phase factor is omitted):

$$a(\bar{x}_3, \bar{x}_1) = A \int \int \exp j [B\bar{x}_2^2 + \Phi(\bar{x}_2) + \bar{x}_2(C\bar{x}_1 + D\bar{x}_3)] d\bar{x}_2,$$

where

$$A = \gamma f / \lambda(f^2 + d_2 f - d_1 d_2); \quad B = \pi d_2 / \lambda(f^2 + d_2 f - d_1 d_2); \\ C = 2\pi / \lambda f; \quad D = 2\pi f / \lambda(f^2 + d_2 f - d_1 d_2);$$

$\gamma$  is a factor that takes into account the brightness of the source;  $\lambda$  is the wavelength of the light wave.

The intensity of the image in the  $x_3 y_3$  plane for the case of an extended incoherent quasimonochromatic source with constant brightness and with the grating oriented in the  $x$  direction, which corresponds to  $\beta = 90^\circ$  in (2.2), has the form

$$I(x_3) = A^2 \int_S \int dx_1 dy_1 g(y_1, y_3) \left| \int_{-b}^b \exp j [Bx_2^2 + \Phi(x_2) + x_2(Cx_1 + Dx_3)] dx_2 \right|_s^2$$

where

$$g(y_1, y_3) = \left| \int_{-b}^b \exp j [By_2^2 + y_2(Cy_1 + Dy_3)] dy_2 \right|_s^2.$$

In practice, the conditions  $(b/f)(\pi d_2/\lambda)^{1/2} \gg 1$  and  $y_{1\max} \ll (b/f)d_2$ , where  $y_{1\max}$  is the size of the source S, are usually satisfied so that  $g = \left| \sqrt{\frac{2}{B}} \exp j \frac{\pi}{4} \right|_s^2$  and the intensity is given by

$$I(x_3) = \frac{2A^2}{B} \int_S \int_S dx_1 dy_1 \left| \int_{-b}^b \exp j [Bx_2^2 + \Phi(x_2) + x_2(Cx_1 + Dx_3)] dx_2 \right|^2, \quad (2.3)$$

The expression obtained permits calculating numerically the intensity in the image plane for a given function  $\Phi(x_2)$  and specific system parameters. Carrying out such calculations repeatedly, for example with the help of a computer, it is possible to find the PCFC only for specific parameters of the optical system (an example of such a calculation is presented in what follows).

3. For a general analysis, it is of interest to have the PCFC in analytic form, even if it is only approximate. Let  $\Phi_m(x_2) < 0.5$ . Then, to within 10%,  $t(x_2) = 1 + j\Phi(x_2)$  and in the F plane the amplitude of the field, which is found by substituting  $d_2 = 0$  in (2.2), equals

$$a(x_F, y_F, x_1, y_1) = -\frac{\gamma}{\lambda f} \int_{-b}^b dy_2 \exp[jCy_2(y_1 + y_3)] \int_{-b}^b dx_2 [1 + j\Phi(x_2)] \exp[jC(x_1 + x_F)x_2].$$

The analytic solution is simplified in examining an idealized optical system, for which  $b \rightarrow \infty$ . Let us assume that the phase grating is described by the function

$$\Phi(x_2) = \sum_k \Phi_k \cos(2\pi\eta_k x_2 + \varphi_k),$$

where  $\Phi_k$ ,  $\eta_k$  and  $\varphi_k$  are the amplitude, frequency, and initial phase of the k-th harmonic component of the oscillations in the phase of the light wave. Then,

$$a(x_F, x_1) = -\gamma\lambda f \delta(y_1 + y_F) \left\{ \delta(x_1 + x_F) + 0.5j \sum_k \Phi_k [\exp(j\varphi_k) \delta \times \right. \\ \left. \times (x_1 + x_F + 2\pi\eta_k C^{-1}) + \exp(-j\varphi_k) \delta(x_1 + x_F - 2\pi\eta_k C^{-1})] \right\}, \quad (3.1)$$

where  $\delta(x, y)$  is a delta function. The amplitude of the field in the image plane for each point of the source is obtained by convoluting the function  $j\lambda^{-1}d_2^{-1}\Psi(x_3, y_3, d_2^{-1})$  with expression (3.1). Taking into account the filtering properties of the  $\delta$ -function, we have, to within terms of order  $\Phi_k^2$ ,

$$I(x_3, x_1, y_1) = \gamma^2 M^2 \left\{ 1 + 2 \sum_k \Phi_k \sin(\pi\lambda f M \eta_k^2) \cos[2\pi M(x_1 + x_3)\eta_k - \varphi_k] \right\}, \quad (3.2)$$

where  $M = fd_2^{-1}$  is a parameter that characterizes the adjustment of the optical system. Integrating (3.2) over the surface of the source S gives

$$I(x_3) = \gamma^2 M^2 \left( S + 2 \sum_k \Phi_k \sin(\pi\lambda f M \eta_k^2) \int_S \int_S \cos[2\pi M \eta_k (x_1 + x_3) - \varphi_k] dx_1 dy_1 \right). \quad (3.3)$$

For a circular source S with radius R, the integral in Eq. (3.3) takes the form

$$\cos(2\pi M \eta_k x_3 - \varphi_k) \int_{-r}^r \sqrt{r^2 - x_1^2} \cos(2\pi M \eta_k x_1) dx_1. \quad (3.4)$$

Since the integral (3.4), after substituting  $xr^{-1} = \sin \omega$ , can be represented as a sum of Bessel functions, after changing  $x_3$  to  $-x_3$  (the picture in the image plane is inverted), the intensity is given by

$$I(x_3) = \gamma^2 M^2 S \left[ 1 + \sum_k K(\eta_k) \cos(2\pi M \eta_k x_3 + \varphi_k) \right], \quad (3.5)$$

where  $K(\eta_k) = 2\Phi_k [J_0(2\pi M r \eta_k) + J_2(2\pi M r \eta_k)] \sin(\rho \lambda f M \eta_k^2)$  is the contrast of the image of the phase grating with spatial frequency  $\eta_k$ .

It is evident from (3.5) that in the optical system being examined, the contrast of the image is linearly related to the amplitude of the phase oscillations (for small amplitudes).

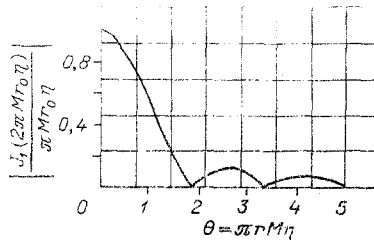


Fig. 2

From (2.1) and (3.5), taking into account the properties of the Bessel functions, it follows that

$$H(\eta) = 2 \frac{J_1(2\pi r M \eta)}{\pi r M \eta} \sin(\pi \lambda f M \eta^2). \quad (3.6)$$

Equation (3.6) describes the PCFC of a direct visualization system with a circular radiation source, assuming that the objectives  $L_1$  and  $L_2$  are properly adjusted, the radiation from the source is quasimonochromatic, and  $\phi_m < 0.5$ . It follows from (3.6) that the PCFC is the product of a slowly varying envelope of the diffraction scattering type and a sinusoidal filler, which depends quadratically on frequency. A graph of the envelope is shown in Fig. 2, where the generalized parameter  $\theta = \pi r M \eta$  is used as the argument. It is evident that the width of the region with relatively large values of PCFC is determined by the adjustment of the system  $M$  and the dimensions of the source  $r$ . From (3.6), functions were derived that permit determining directly the minimum  $T_{\min}$  and maximum  $T_{\max}$  periods of the harmonic components of the nonuniformities visualized by the system (the threshold value of the PCFC is taken as equal to 0.2 of the maximum), for a number of values of the focal length of the lens  $L_2$  (0.032, 0.32, 0.64, 1.28, and 1.92 m correspond to the curves 1-5 in Fig. 3) and of the source diameter (0.1, 0.2, and 0.4 mm correspond to curves 6-8 in Fig. 3):  $T_{\min} \approx 2rM$ ,  $T_{\max} \approx \sqrt{20\pi\lambda f M}$ . It follows from Fig. 3 that in order to create a wide band system it is necessary to strive to decrease the diameter of the radiation source and to increase the focal length of the lens  $L_2$ .

4. In order to study the frequency selection properties of the direct schlieren method for cases when the conditions assumed in deriving (3.6) are not satisfied, we carried out computer calculations using Eq. (2.3) directly. We calculated the distribution of the illumination for phase modulation amplitudes equal to 0.1 and 1 rad. The calculations were carried out for a square  $50 \times 50 \mu\text{m}$  source with  $\lambda = 0.5 \mu\text{m}$  and a lens with a diameter of 80 mm and focal length of 640 mm with an adjustment of  $M = 21.4$ . The input function was given at steps of 0.2 or 0.1 mm depending on the input frequency, which permitted studying the properties of the system up to frequencies of  $10 \text{ mm}^{-1}$ . In calculating the integral in (2.3), the quadratic function  $Bx_2^2$  was approximated by straight-line segments on intervals of length 0.2 mm, which was a completely acceptable discretization, since a decrease in the step-size to 0.004 mm changed the result by only 1%.

The results of the calculations are presented in Fig. 4 in the form of graphs of the contrast  $K$  as a function of the spatial frequency  $\eta$  for two values of the amplitude of the phase oscillations:  $\phi_m = 1$  rad (curve 1) and  $\phi_m = 0.1$  rad (curve 3); the corresponding functions  $K(\eta)$ , computed using the approximate equation (3.5) with  $K(\eta)$  further multiplied by the function  $\varphi(\phi_m)$  and the Bessel function replaced by a sinusoidal function with the same argument (since the source has a square shape), are presented in Fig. 4 as well (curves 2 and

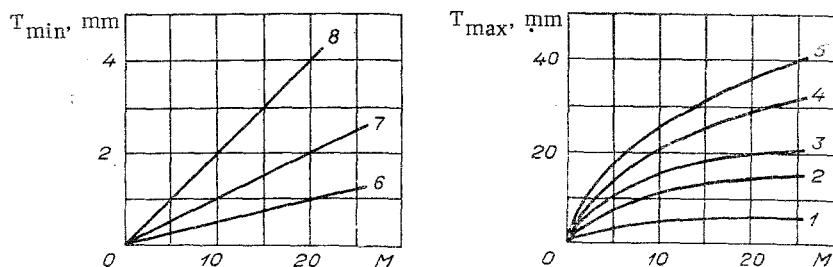


Fig. 3

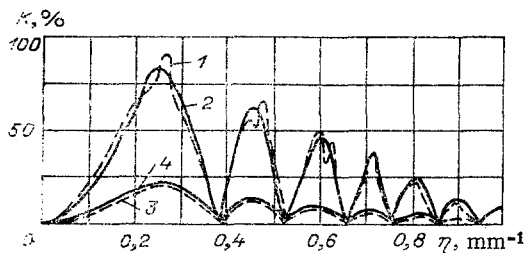


Fig. 4

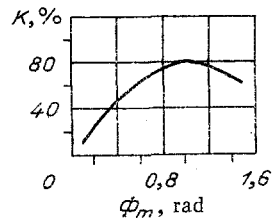


Fig. 5

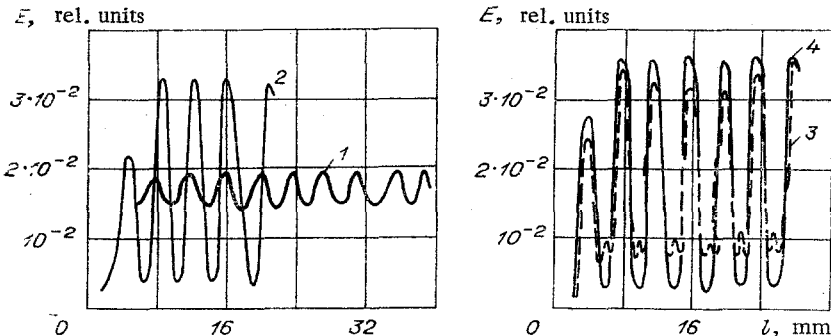


Fig. 6

4); the factor  $\varphi(\Phi_m)$  is introduced in order to take into account the nonlinearity of the system, which is especially important for contrasts close to 100%. In order to determine this factor, we calculated the dependence of the contrast of the phase grating image with frequency  $0.24 \text{ mm}^{-1}$  (close to the frequency of the first maximum for the design parameters of the system) on the phase modulation amplitude (Fig. 5). It follows from Fig. 4 that the contrast calculated using the exact and approximate equations agrees well with amplitude modulation of 0.1 rad. The differences are also insignificant for  $\Phi_m = 1 \text{ rad}$  (in taking into account the nonlinearity). Figure 6 shows curves of the distribution of illumination  $E$  for a frequency of  $0.24 \text{ mm}^{-1}$  and a number of values of the modulation amplitude (0.1, 0.7, 1.5, and 1 rad in curves 1-4, respectively). It is evident from Fig. 6 that with a modulation amplitude of 1.5 rad (curve 3), large distortions begin to appear in the image of the phase grating.

The results presented allow the experimentalist to optimize the parameters of the optical system that realizes the direct schlieren method, used for studying turbulent fields with different spectral content, and to take into account the features arising in visualizing the nonuniformities stemming from spatial frequency selectivity of the method, in analyzing the results of measurements.

#### LITERATURE CITED

1. S. R. Stefanov, A. M. Trokhan, and Yu. D. Chashechkin, "Investigation of turbulent pulsations in the index of refraction of water using a Töpler instrument," *Zh. Prikl. Mekh. Tekh. Fiz.*, No. 5 (1971).
2. Yu. I. Kopilevich, "Relation between the characteristics of the signal in a schlieren instrument and the turbulence spectrum," *Zh. Prikl. Mekh. Tekh. Fiz.*, No. 6 (1975).
3. Yu. I. Kopilevich, "Reconstruction of the turbulence spectrum from the temporal characteristics of the signal from a schlieren instrument," *Zh. Prikl. Mekh. Tekh. Fiz.*, No. 1 (1978).
4. B. V. Naumov, "Transfer characteristic and the sensitivity of a photoelectric schlieren instrument," *OMP*, No. 10 (1970).
5. A. G. Polishchuk, "Visualizing the shape of the wave front using a schlieren instrument with subtraction," *Avtometriya*, No. 5 (1977).
6. M. M. Skotnikov, *Quantitative Schlieren Methods in Gas Dynamics* [in Russian], Nauka, Moscow (1976).
7. *Optical Analytical Methods in a Ballistics Experiment* [in Russian], Nauka, Leningrad (1979).

8. Yu. N. Kalugin, É. I. Krasovskii, and B. V. Naumov, "Increasing the accuracy of instruments for studying the anisotropy of turbulence" in: Third All-Union Conference on Experimental Methods and Apparatus for Studying Turbulence, Abstracts of Reports [in Russian], Izd. Inst. Termofiz. Sib. Otd. Akad. Nauk SSSR, Novosibirsk (1979).
9. D. Holder and R. Nort, Schlieren Methods in Aerodynamics [Russian translation], Mir, Moscow (1966).
10. V. M. Kamenkovich and A. S. Monin (editors), Physics of the Ocean [in Russian], Nauka, Moscow (1978), Vol. 1.
11. A. I. Williams, "Images of ocean microstructure," Deep-Sea Res., 22, 811 (1975).
12. G. Stroke, Introduction to Coherent Optics and Holography, Academic, New York (1966).
13. A. Marechal and M. Franson, Structure of an Optical Image [Russian translation], Mir, Moscow (1964).
14. R. Collier, K. Berkhardt, and L. Lin, Optical Holography, Academic, New York (1971).

EXPERIMENTAL INVESTIGATION OF NONSTATIONARY HEAT TRANSFER IN  
A POROUS LAYER WITH A LIQUID PERCOLATING IN THE LAYER

V. A. Mukhin and N. N. Smirnova

UDC 536.242

The solution of problems involving heat and mass transfer in porous layers is distinguished by great complexity. This complexity stems from the hydrodynamic and thermal interaction of the percolating flow with the medium filling the layer and with the surrounding mass (or channel walls).

At the present time, several approaches are available for solving such problems. A widely used model of such a flow is one in which it is assumed that the thermal resistance of the solid particles that make up the layer is small, i.e., a certain homogeneous medium is examined in which the actual characteristics of a nonuniform medium are replaced by equivalent characteristics. Such a model of the flow is used in [1-3] and in other studies. In another approach [4, 8], the thermal resistance of the elements of the layer is taken into account and the basic equations become integrodifferential equations. These equations are solved in terms of series and complicated integrals. Calculations based on the solutions obtained in complicated physical situations become difficult.

Recently, a solution has been proposed for this problem involving a nonstationary temperature field in a porous stratum based on reduction of the integrodifferential equation to an equivalent heat conduction equation [5].

The purpose of the present work is to check different theories and the equivalent heat conduction equation method.

An experimental setup was prepared for studying nonstationary heat exchange with percolation of a liquid in a porous medium. The basic element of the setup was a cylindrically-shaped tank with a diameter of 0.6 m and height 0.6 m with a removable cover. The tank was filled with small glass spherules with various diameters. In order to establish uniform percolation, a parallelepiped was separated out in the center of the volume with length, width, and height dimensions equal to 0.3, 0.42, and 0.44 m, respectively. The volume that was separated out was isolated from the surrounding mass from below, above, and on all sides with the help of a thin sheet of vinyl plastic, which is a material that has a low thermal conductivity. A fluid was introduced into one side of the isolated volume and removed from the other side. The liquid was introduced through perforated pipes with diameter  $d = 10^{-2}$  m with a long perforated part equal to the height of the isolated volume. These pipes were distributed uniformly over the entire depth of the inlet and outlet cross sections with a step of  $5 \cdot 10^{-2}$  m. The perforated pipes were connected with collectors outside the isolated volume. A frame containing 25 nichrome-constantan thermocouples (five rows distributed over